

Research

Open Access

Neuronal apoptosis and inflammatory responses in the central nervous system of a rabbit treated with Shiga toxin-2

Kiyomi Takahashi*¹, Nobuaki Funata², Fusahiro Ikuta³ and Shigehiro Sato¹

Address: ¹Department of Microbiology, Iwate Medical University School of Medicine, 19-1 Uchimaru, Morioka, Iwate 020-8505, Japan,

²Department of Pathology, Tokyo Metropolitan Komagome Hospital, 3-18-22 Honkomagome, Bunkyo-ku, Tokyo 113-8677, Japan and ³Niigata Neurosurgical Hospital and Brain Research Center, 3057 Yamada, Niigata, Niigata 950-1101, Japan

Email: Kiyomi Takahashi* - kiyomit@iwate-med.ac.jp; Nobuaki Funata - funata-k@komagome-hospital.bunkyo.tokyo.jp;

Fusahiro Ikuta - ikuta@muse.ocn.ne.jp; Shigehiro Sato - ssato@iwate-med.ac.jp

* Corresponding author

Published: 21 March 2008

Received: 4 February 2008

Journal of Neuroinflammation 2008, 5:11 doi:10.1186/1742-2094-5-11

Accepted: 21 March 2008

This article is available from: <http://www.jneuroinflammation.com/content/5/1/11>

© 2008 Takahashi et al; licensee BioMed Central Ltd.

This is an Open Access article distributed under the terms of the Creative Commons Attribution License (<http://creativecommons.org/licenses/by/2.0>), which permits unrestricted use, distribution, and reproduction in any medium, provided the original work is properly cited.

Abstract

Background: Shiga toxins (Stxs) are the major agents responsible for hemorrhagic colitis and hemolytic-uremic syndrome (HUS) during infections caused by Stx-producing *Escherichia coli* (STEC) such as serotype O157:H7. Central nervous system (CNS) involvement is an important determinant of mortality in diarrhea associated-HUS. It has been suggested that vascular endothelial injuries caused by Stxs play a crucial role in the development of the disease. The current study investigates the relationship between the cytotoxic effects of Stxs and inflammatory responses in a rabbit brain treated with Stx2.

Methods: In a rabbit model treated with purified Stx2 or PBS(-), we examined the expression of the Stx receptor globotriaosylceramide (Gb3)/CD77 in the CNS and microglial activation using immunohistochemistry. The relationship between inflammatory responses and neuronal cell death was analyzed by the following methods: real time quantitative reverse transcriptase (RT)-polymerase chain reaction (PCR) to determine the expression levels of pro-inflammatory cytokines, and the terminal deoxynucleotidyl transferase (TdT)-mediated dUTP nick-end labeling (TUNEL) method to detect apoptotic changes.

Results: Gb3/CD77 expression was detected in endothelial cells but not in neurons or glial cells. In the spinal cord gray matter, significant levels of Gb3/CD77 expression were observed. Severe endothelial injury and microvascular thrombosis resulted in extensive necrotic infarction, which led to acute neuronal damage. Conversely, in the brain, Stx receptor expression was much lower. The observed neuropathology was less severe. However, neuronal apoptosis was observed at the onset of neurological symptoms, and the number of apoptotic cells significantly increased in the brain at a later stage, several days after onset. Microglial activation was observed, and tumor necrosis factor (TNF)- α and interleukin (IL)-1 β mRNA in the CNS parenchyma was significantly up-regulated. There was significant overexpression of TNF- α transcripts in the brain.

Conclusion: This study indicates that Stx2 may not directly damage neural cells, but rather inflammatory responses occur in the brain parenchyma in response to primary injury by Stx2 in vascular endothelial cells expressing Gb3/CD77. These findings suggest that neuroinflammation may play a critical role in neurodegenerative processes during STEC infection and that anti-inflammatory intervention may have therapeutic potential.

Background

Shiga toxin (Stx)-producing *Escherichia coli* (STEC), such as serotype O157:H7, produces 1 or both of the 2 antigenically distinct toxins Stx1 and Stx2 [1]. These toxins in the circulation of patients infected with STEC are the major cause of hemorrhagic colitis and the hemolytic-uremic syndrome (HUS) associated with the prodrome of diarrhea [2]. The extent and severity of extrarenal involvement, particularly the neurological impairment, are important determinants in the poor prognosis of STEC-associated HUS patients [3]. Pathological examination has shown that endothelial injury of small vessels and microvascular thrombosis are the prominent changes occurring in multiple organs, including the CNS [2,3]. Animal models treated with Stx1 [4,5] or Stx2 [6], also develop neurological symptoms and exhibit similar neuropathology. Stx1- or Stx2-binding was immunohistochemically demonstrated in small vessels and/or the subsets of some cells in the lesions, but not in the neurons [4,7].

Stx1 and Stx2 are AB₅ holotoxins that consist of an enzymatic A subunit and 5 copies of a binding B subunit [8]. The B subunits specifically bind to the terminal [Gal(1-4)Gal] disaccharides of the receptor Gb3/CD77 consisting of a trisaccharide β -linked ceramide (globotriaosylceramide) that is expressed on the cell membrane [9,10]. Stxs are then internalized with Gb3/CD77 and retrogradely transported from the endosomes through the *trans*-golgi network and golgi apparatus to the endoplasmic reticulum [9]. The A subunit of the toxin is then cleaved and translocated into the cytosol; it then inhibits host cell protein synthesis by RNA N-glucosidase activity, resulting in cell death [10]. Recent studies have reported that cell death occurs by apoptosis [11,12]. Toxin-binding to Gb3/CD77 is the primary determinant of the cytotoxic and pathological effects of Stxs. However, Gb3/CD77 expression in the CNS parenchyma has not been well examined, except in the dorsal root ganglia (DRG) [13]. Furthermore, the direct cytotoxic actions of Stxs against neurons and glial cells remain unclear.

CNS responses to a variety of insults incorporate a wide spectrum of cellular responses that include microglial activation [14,15] and local production of endogenous molecules such as pro-inflammatory cytokines, reactive oxygen, and nitrogen species that affect neuronal integrity [reviewed in [16] and [17]]. These inflammatory responses in the CNS are now recognized to play a critical role in the pathogenesis and progression of acute and chronic neurodegenerative diseases, including stroke [18], Alzheimer's disease [19,20], Parkinson's disease [21], and viral infection [22,23]. It has been demonstrated that pro-inflammatory cytokines, particularly TNF- α , induce neuronal apoptosis in human brain cell cultures and animal

models through TNF/TNF receptor signaling [24,25] and further production of other inflammatory and/or neurotoxic molecules [19,21]. Administration of TNF- α to mice infected with *Escherichia coli* O157:H7 modified the neurological signs and pathology [26]. In the case of neurological impairment during STEC infection, however, little is known about the relationship between inflammatory responses in the CNS due to the toxin and the neurodegenerative events in either patients or animal models.

In the current study, we showed the regional distribution and cellular localization of Gb3/CD77 expression in the CNS parenchyma of a rabbit model in order to examine whether the toxins are able to directly injure neuronal cells. Further, we investigated the relationship between neuropathology and the interaction of toxin with Gb3/CD77 and that between inflammatory processes in the CNS and neuronal cell death in rabbits treated with Stx2.

Materials and methods

Toxin and animals

The Stx2 preparation was kindly provided as described previously [27] by Denka Seiken Co., Ltd., (Niigata, Japan). The same lot of toxin was used for all experiments in this study. The protein content of the toxin was 130 μ g/ml as determined by Bradford method. The endotoxin content was 34.5 pg/ml as measured by a limulus test (ES-Test Wako Kit), using computerized turbidimetric equipment (Wako Chemical Industries, Co. Ltd, Osaka, Japan) [28]. Biological activity of Stx2 assessed by cytotoxicity on Vero cells was found to be 5×10^6 CD₅₀/ μ g protein.

Japanese male white rabbits (Japan SLC, Inc., Hamamatsu, Japan) weighing 2.2 to 2.4 kg were used throughout the experiments. All protocols used in this study were in accordance with the Guidelines for Animal Experiments of Iwate Medical University. Animals were acclimated to standard laboratory conditions with free access to rabbit chow and water. In each experiment, at least 2 rabbits per group were used. The toxin was injected into the left marginal ear vein in a single bolus. Six doses of 0.1 to 4.0 μ g/kg body weight of Stx2 were administered for clinical evaluation. For other experiments, including histopathological examination and gene expression, 2.5 μ g/kg of toxin were administered by the same route. Controls were untreated rabbits injected with PBS(-) as above.

Laboratory tests

Blood samples were collected before administration of Stx2 and at the onset of paralysis. Hematology, blood urea nitrogen, creatinine, alanine aminotransferase, aspartate aminotransferase, and amylase were measured by standard laboratory procedures in our hospital. The presence of blood in stools was tested using the Occult Blood Slide 5 Kit (Shionogi & Co., Ltd., Osaka, Japan).

Tissue preparation

Animals were intravenously injected with a lethal dose of pentobarbital sodium and then rapidly perfused with sterile physiological saline transcardially, followed by 2% paraformaldehyde (PFA). Brain that denote the cerebrum, midbrain, cerebellum and brain stem, spinal cord with root ganglia and nerve fibers were removed and post-fixed with 4% PFA overnight at 4°C. The tissue was paraffin-embedded and sliced at 5 µm for histopathology, immunohistochemistry, and the terminal deoxynucleotidyl transferase (TdT)-mediated dUTP nick end-labeling (TUNEL) assay. For the immunofluorescence assay (IFA) tissue blocks were freshly embedded and frozen after cryoprotection as described previously [29]. Tissue blocks were stored at -70°C until sectioning.

Immunohistochemistry

Localization of Gb3/CD77 was examined by IFA. Cryosections cut at 7 µm were fixed with 4% PFA for 10 min immediately prior to IFA and incubated with anti-human CD77 rat IgM antibody [13] (1:100 dilution, Beckman Coulter, Inc., Fullerton, CA) or with rat IgM isotype as a negative control (1:100 dilution, Beckman Coulter) for 24~96 hrs at 4°C, followed by reaction with anti-rat IgM goat IgG F(ab)₂ antibody-FITC conjugate (1:200 dilution, Beckman Coulter) for 30 min at room temperature. To examine the cellular localization of Gb3/CD77, double-staining with rhodamine conjugated *Ricinus communis* agglutinin I (RCA 120) (1:5,000 dilution, Vector Laboratories, Inc., Burlingame, CA) was carried out overnight at 4°C on the same sections after Gb3/CD77 detection. The sections were observed with the LSM 510 confocal laser scanning microscopy (Carl Zeiss, Oberkochen, Germany).

Paraffin-embedded sections were stained for microglial cells as described previously [23,30], with some modification. Briefly, deparaffinized sections were pretreated with 3% H₂O₂ for 10 min to quench the endogenous peroxidase activity, and were then incubated with biotinylated RCA 120 (1:3,000 dilution) or *Griffonia simplicifolia* lectin I-B4 isolectin (GSL I-B4) (1:2,000 dilution, Vector) overnight at 4°C. This was followed by a reaction with peroxidase conjugated streptavidin (DAKO). The color reaction was performed using 0.5 mg/ml of diaminobenzidine (DAB) (Sigma-Aldrich, Inc., St. Louis, MO) substrate solution with 0.02 % of H₂O₂. Sections were counterstained with methyl green and mounted.

TUNEL assay

In order to detect *in situ* DNA fragmentation, the TUNEL assay was performed using the *In situ* Apoptosis Detection Kit (Takara Bio Inc., Otsu, Japan) according to the manufacturer's protocols. Briefly, deparaffinized sections were permeabilized with proteinase K (DAKO) and treated with 3% H₂O₂ as above. Sections were incubated with

Labeling Safe Buffer, i.e. an end-labeling mixture containing FITC-conjugated dUTP and TdT Enzyme, at 37°C for 60 min. Tissue sections were reacted with anti-FITC horseradish peroxidase-conjugated antibody for 30 min at 37°C. Color reaction with DAB was performed, followed by counterstaining with methyl green as above. TUNEL assay controls included omission of TdT and sections from rabbits (n = 2) treated with PBS (-). To estimate apoptotic cell death quantitatively, tissue sections of rabbits treated with 2.5 µg/kg of Stx2 were examined at the onset and at a later stage several days after onset (n = 2 in each group). Apoptotic cells in 16 to 50 fields and TUNEL-positive vessels in 140 to 160 fields were counted at 100× magnification in 3 sections from each region of the brain parenchyma.

Real-time quantitative reverse transcription-polymerase chain reaction

Total RNA was extracted from 12 regions of the CNS using NucleoSpin RNA II (Macherey-Nagel GmbH & Co. KG, Düren, Germany) and 1 µg of total RNA was used for cDNA synthesis with oligo dT and MMLV-RT (Invitrogen Corp., Carlsbad, CA). Two µl of each cDNA product was subjected to TNF-α and IL-1β mRNA quantitation using SYBR Green PCR Master Mix [31] and an ABI PRISM 7700 Sequence Detection System (SDS) (Applied Biosystems, Foster City, CA), followed by a dissociation curve analysis and subsequent agarose gel electrophoresis to confirm amplification specificity. The following primer sets were used: TNF-α (size, 243 bp; melting temperature (T_m), 87.5°C), forward [32]: 5'-AGCCCACGTAGTACCAAACCC-3', reverse: 5'-GAGAGGAGGTTGACCTTGTT-3' [GenBank: [M12485](#) and [M12486](#)]; IL-1β (size, 264 bp; T_m, 81.0°C), forward [33]: 5'-GAATCTGAACCAACAAGTGG-3', reverse: 5'-ATGTACCAGTTGGGGAAC-3' [GenBank: [M26295](#)]; and GAPDH was used as an endogenous reference (size, 308 bp; T_m, 88.3°C), forward: 5'-TCTCTCAAGATTGTCAGCAA-3', reverse: 5'-AGGTCCACGACCGACACGTT-3' [GenBank: [L23961](#)]. All experiments were carried out twice in triplicate, amplification plots were analyzed using the ABI Prism 7700 SDS version 1.7 software. Expression levels of mRNA were quantified by the relative standard curve method, according to the User Bulletin #2 for ABI Prism 7700 SDS. Briefly, the target amount was divided by the endogenous reference (GAPDH) amount to obtain a normalized target value for each sample. The relative quantity of cytokine mRNA levels was calculated by dividing each of the normalized target values by the normalized calibrator value for each sample, and was expressed as *n*-fold difference and mean ± SD. CNS samples from control rabbits treated with PBS(-) were used as calibrators in this study.

Statistics

Mean \pm SEM or mean \pm SD were determined, and to compare mean values in 2 separate groups, Student's *t*-test was used. Values of $P < 0.05$ were considered to be significant.

Results

Clinical findings and laboratory studies

In all rabbits injected with 0.1 to 4.0 $\mu\text{g}/\text{kg}$ of Stx2, digestive symptoms such as anorexia, weight loss, and diarrhea were observed (Table 1). The 50% lethal dose was 0.79 $\mu\text{g}/\text{kg}$, and neurological symptoms developed in 2 of 4 rabbits (50%) injected with 1.0 $\mu\text{g}/\text{kg}$ of Stx2 and in 5 of 6 (83.3%) treated with 2.0 to 4.0 $\mu\text{g}/\text{kg}$ of toxin (Table 1). As early as 28~42 h after injection, among the 23 animals injected with 1.0 to 4.0 $\mu\text{g}/\text{kg}$ (including the 16 in table 1), 18 showed neurological symptoms, which included mild gait disturbance in 2 animals and paralysis in 16 rabbits. There were no significant changes in the hematological and blood biochemical values at the onset of neurological symptoms when compared with those obtained before administration of the toxin (not shown), except for a slight elevation in the leukocyte count (8345 ± 394 and 9602 ± 755 , before administration and at the onset of neurological symptoms, respectively).

Gb3/CD77 expression and histopathological evaluation

Regional distribution and cellular localization of Gb3/CD77

Specific and intense fluorescence signals were strongly detected on the blood vessels of the spinal cord gray matter (Fig. 1A). Whereas the intensity of fluorescence was weaker in the white matter of the spinal cord (Fig. 1B), root ganglia (not shown), and brain parenchyma (Fig. 1C). Signals were negative in the control sections incubated with rat IgM isotype antibody (not shown). Double staining with rhodamine-conjugated RCA 120, which recognizes and specifically binds to terminal [D-Gal β (1-4)-D-GlcNAc] disaccharides [34], demonstrated different fluorescence signal patterns from Gb3/CD77 and revealed colocalization of both in the small vessels and capillaries (Fig. 1D to 1F); however, this was not evident in other subsets of cells in the CNS parenchyma.

Spinal cord

The prominent pathological damage was massive necrotic infarction in irregular form, which was mostly noted in the gray matter of the cervical and lower thoracic to lumbar cords (Fig. 2A). In and around the ischemic lesions, neuronal bodies were damaged and axons were swollen. Small vessels and capillaries were frequently injured and occluded by fibrin-like thrombi (Th in Fig. 2B) and some exhibited eosinophilic exudates (dV) or microscopic hemorrhage (mH) as shown in Fig. 2B. In a rabbit with mild ataxic gait but not paralysis, thrombi and/or microscopic hemorrhage were only observed in the nerve roots. Some axons were swollen and some of these were degenerated or lost (Fig. 2C), neurons in the DRG exhibited normal appearance (not shown).

Brain parenchyma

In contrast to the severe ischemic damages in the spinal cord, a few foci of microscopic hemorrhage (Fig. 2D) and/or ischemic lesions were scattered in the brain parenchyma and fibrin-like thrombi were often observed (Th) in small vessels and capillaries at the onset of symptoms. Neurons were damaged in the basal ganglia (Fig. 2E) and thalamus at onset. These cells showed atrophy and darkly stained cytoplasm. Several days after onset, at a later stage, some neurons in CA1 of the rabbit hippocampus morphologically exhibited an apoptotic appearance such as condensed and fragmented nuclei in shrunken cytoplasm (Fig. 2F).

Vascular damages

Elastica-Goldner staining showed that small vessels in the infarction lesions in the spinal cord gray matter were mainly damaged (Fig. 3A) and occluded by fibrin-like thrombi (Th). Platelet thrombi (arrow in Fig. 3A) or fragmented red blood cells (arrow head in Fig. 3A) were also present in a few vessels. Arterioles in the spinal cord showed endothelium with pycnotic nuclei and swollen cytoplasm as well as thickening of the vessel wall, but not formation of thrombi (Fig. 3B). These vascular damages were less severe in the brain parenchyma. Phosphotungstic acid hematoxylin (PTAH) staining revealed that most of the thrombi in small vessels and exudates or precipi-

Table 1: Dosage range of Stx2 and clinical findings

Dose ($\mu\text{g}/\text{kg}$)	neurological symptoms (%)	Diarrhea/occult blood	Body weight loss (%)
0.1	1 ^a /5 (20)	--+/--+	8.0~38.8
0.25	0/4 (0)	+/+	13.2~25.6
0.5	0/4 (0)	+/+	22.0~36.7
1.0	2/4 (50)	+/+	26.7
2.0	5/6 (83.3)	+/+	- ^b
4.0	5/6 (83.3)	+/+	- ^b

^aTransient gait disturbance was observed on the 4th to 6th day after administration of Stx2.

^bnot measured.

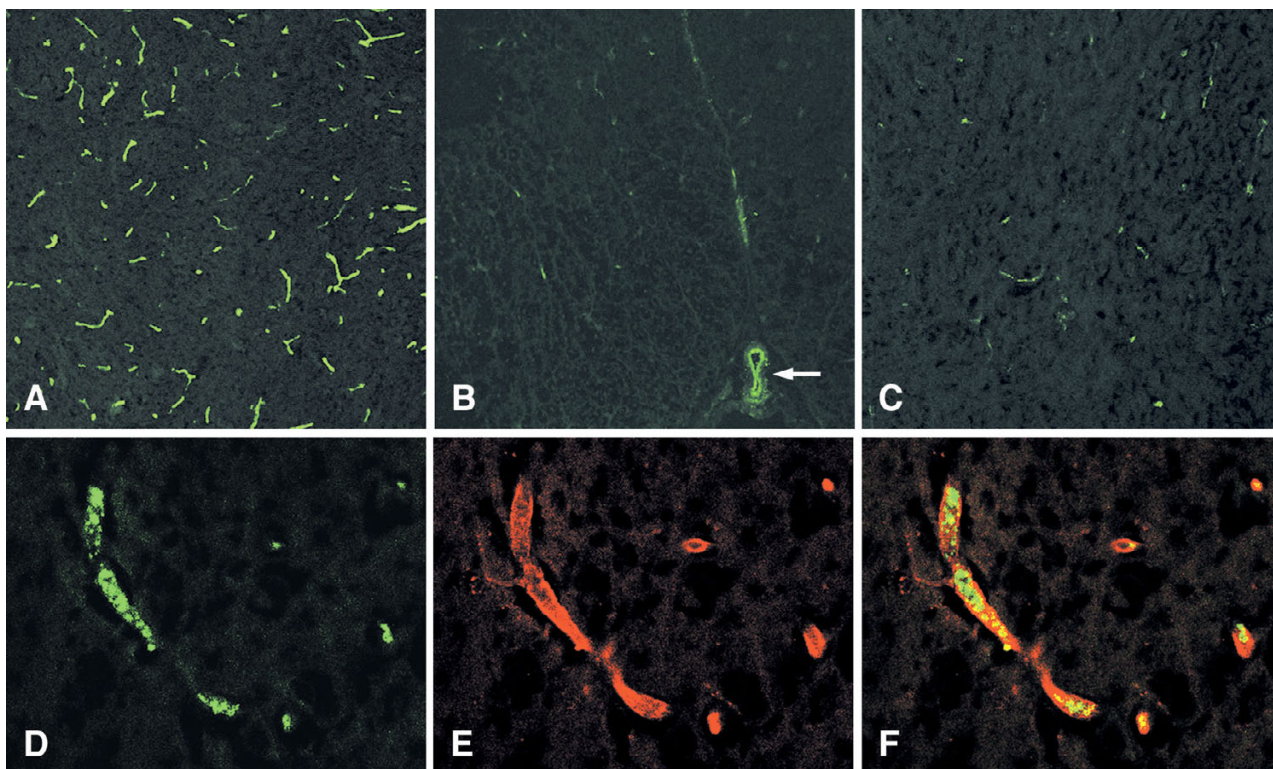


Figure 1

Immunofluorescence analysis of the localization of Stx receptor Gb3/CD77 in the rabbit CNS. Intense fluorescence was detected on the blood vessels of the spinal cord gray matter (A), whereas fluorescent signals were much weaker on those of the spinal cord white matter except anterior spinal artery (arrow) (B) and hippocampus (C). Confocal images of double staining with rhodamine conjugated RCA 120 showed the different fluorescence signal patterns from Gb3/CD77 and revealed the colocalization of both in the small vessels and capillaries; Gb3/CD77 (D), RCA 120 (E), and merged (F). (Original magnification: (A)-(C) 200 \times ; (A)-(E) 630 \times)

tates around capillaries were formed with fibrin in both the spinal cord (Fig. 3C) and brain parenchyma.

Apoptotic cell death of neuronal cells and endothelial cells in the brain parenchyma

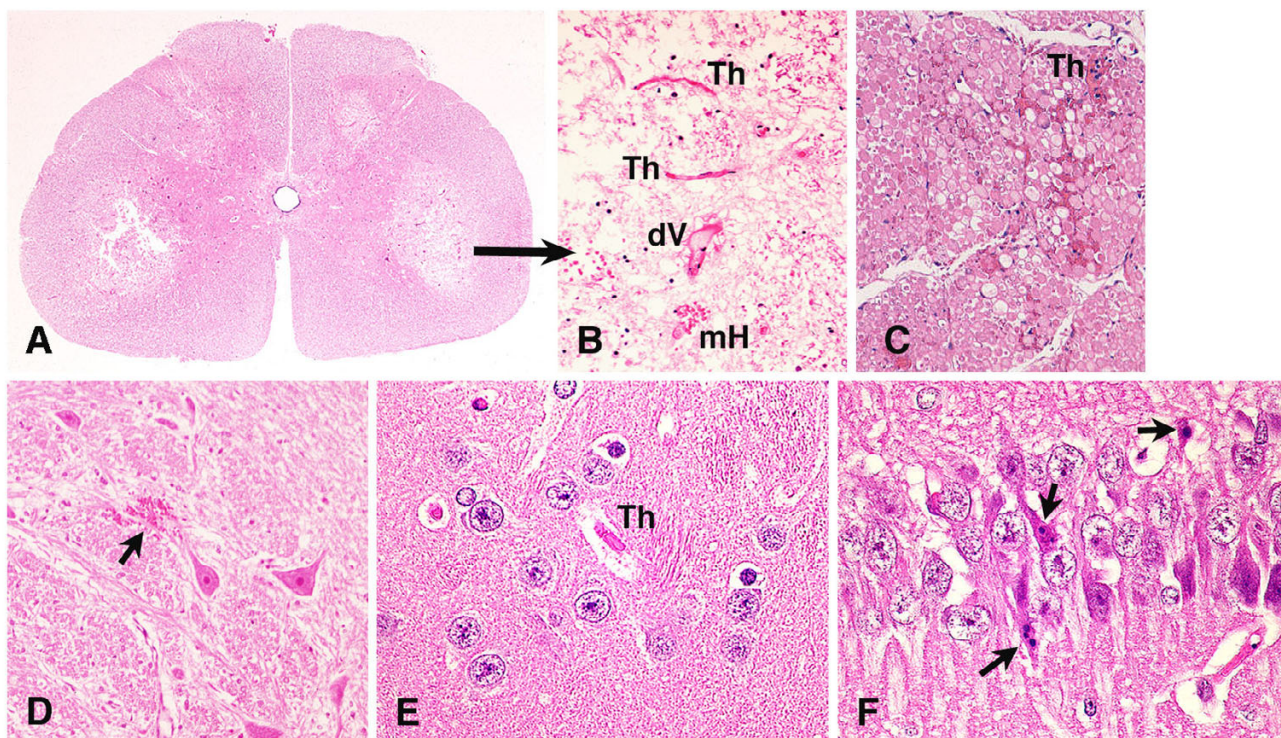
At the onset of paralysis, apoptotic granular neurons with condensed brown DAB precipitate were observed in the dentate gyrus of the hippocampus (Fig. 4A) and granular layers of the cerebellum. TUNEL-positive neurons with apoptotic bodies increased at a later stage several days after onset in the pyramidal neurons in CA1 of the hippocampus (Fig. 4B). Apoptotic changes were also observed diffusely in neurons in other cerebral regions, namely, the basal ganglia, thalamus and cerebral cortex (Fig. 4C), among glial cells in the pons (Fig. 4D), and in some endothelial cells of the small vessels and capillaries in the cerebrum (Fig. 4E). TUNEL assay with omission of TdT (Fig. 4F) was negative in all the regions. The number of apoptotic cells per 10 fields (Fig. 4G) and of TUNEL-positive vessels per 100 fields (Fig. 4H) at onset or at a

later stage were compared with those of control rabbits treated with PBS(-). In the hippocampus, apoptotic neurons were significantly elevated at both onset (53.1 ± 3.49) and a later stage (94.0 ± 7.65), ($P < 0.01$). Apoptotic cells in the granular layers of the cerebellum (75.9 ± 4.76 , $P < 0.05$), other cerebral regions, including the basal ganglia, thalamus and cerebral cortex (74.1 ± 4.04 , $P < 0.01$), and TUNEL-positive vessels (88.2 ± 23.74 , $P < 0.05$) were significantly increased at a later stage.

Inflammatory responses in CNS

Microglial activation

At the onset of paralysis, intense GSL I-B4 staining of microglial cells were diffusely observed in both the spinal cord and brain. Microglial activation was obvious due to the morphological change in the cells. Activated microglia were markedly found in and around ischemic lesions in the spinal cord (Fig. 5A) and extensively increased in the brain parenchyma (Fig. 5B). A large number of microglia exhibited an amoeboid form when compared with the ram-

**Figure 2**

Neuropathology in the rabbits treated with 2.5 µg/kg Stx2 (H&E staining). (A) The lower segment of the lumbar spinal cord showed extensive necrotic infarction in the gray matter at the onset of severe paraplegia. (B) Higher magnification of ischemic lesions in the panel (A), small vessels with fibrin-like thrombi (Th), degenerated vessels (dV), and microscopic hemorrhage (mH) were observed. (C) Nerve roots of the rabbit with ataxic gate showed microvascular thrombi and microscopic hemorrhage. Some nerve fibers were swollen and/or degenerated. In contrast to the spinal cord, (D) microscopic hemorrhage (arrows) were scattered in the brain parenchyma. At a later stage, neurons in the basal ganglia showed atrophy, darkly stained cytoplasm (E), and in the hippocampus some pyramidal neurons morphologically showed apoptotic changes with shrunken cytoplasm and apoptotic bodies (arrows) (F). (Original magnification: (A) 5.2×; (B) 250×, (C) and (D) 100×, (E) and (F) 400×.)

ified form in the control sections of the spinal cord and brain parenchyma (Fig. 5C and 5D, respectively). Interestingly, microglial activation greatly increased before the onset of neurological symptoms, as early as 6 to 12 h after Stx2 injection and was also observed at a later stage.

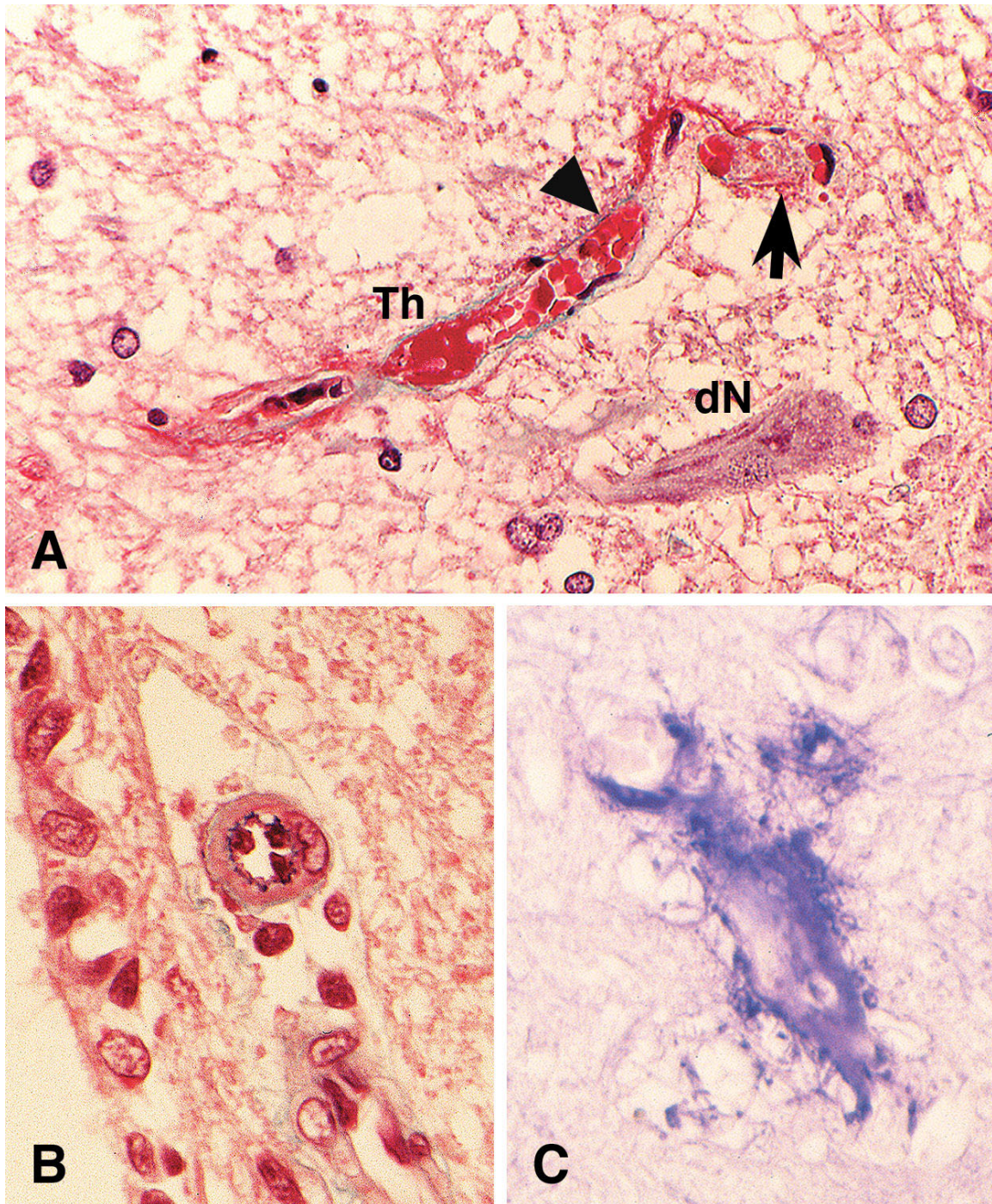
Up-regulation of pro-inflammatory cytokine mRNA

Since microglial activation was observed before onset, the expression levels of pro-inflammatory cytokine mRNA were examined 24 h after administration of 2.5 µg/kg Stx2 (n = 2) in the frontal area, basal ganglia, hippocampus, thalamus, temporal cortex, midbrain, cerebellum, pons and medulla, cervical, thoracic and lumbar spinal cord, and compared to the expression levels in the same regions of rabbits injected with PBS(-) as a calibrator (n = 2). Expression levels of TNF-α (Fig. 6A) and IL-1β (Fig. 6B) mRNA increased in all regions of the rabbits treated with Stx2 although the neurological signs had not developed at

this time point. TNF-α transcripts were substantially up-regulated (by $15.55 \pm 1.66 \sim 128.53 \pm 13.54$ fold increase) and particularly overexpressed in 4 regions of the cerebrum, namely, the basal ganglia, hippocampus, thalamus, and cerebral cortex (128.53 ± 13.54 , 107.35 ± 10.05 , 106.73 ± 8.35 , 93.65 ± 3.76 fold, respectively); TNF-α expression also greatly increased in the cerebellum (51.62 ± 4.43 fold). Whereas the IL-1β mRNA levels were moderately increased (by $2.63 \pm 0.30 \sim 12.14 \pm 0.68$ fold), except in the hippocampus (27.60 ± 1.71 fold). Comparable results were obtained using different set of rabbits.

Discussion

The present study demonstrated that in the brain of rabbits treated with purified Stx2, neurodegenerative events coincide with inflammatory responses characterized by microglial activation and production of pro-inflammatory cytokines. In addition, these events greatly differed

**Figure 3**

Vascular degeneration in the rabbits treated with 2.5 µg/kg Stx2. **(A)** In the infarction lesions in spinal cord gray matter, small vessels were damaged with extravascular exudates and occluded with fibrin-like (Th) and platelet (arrow) thrombi and with fragmented erythrocytes (arrow head). Some arteries and arterioles **(B)** in the spinal cord showed an endothelium with pycnotic nuclei and swollen cytoplasm as well as thickening of the vessel walls. **(C)** PTAH staining indicated that most of the thrombi and exudates or precipitates around the capillaries were formed with fibrin in both the spinal cord and brain parenchyma. **(A) & (B):** Elastica-Goldner staining. (Original magnification: 400×)

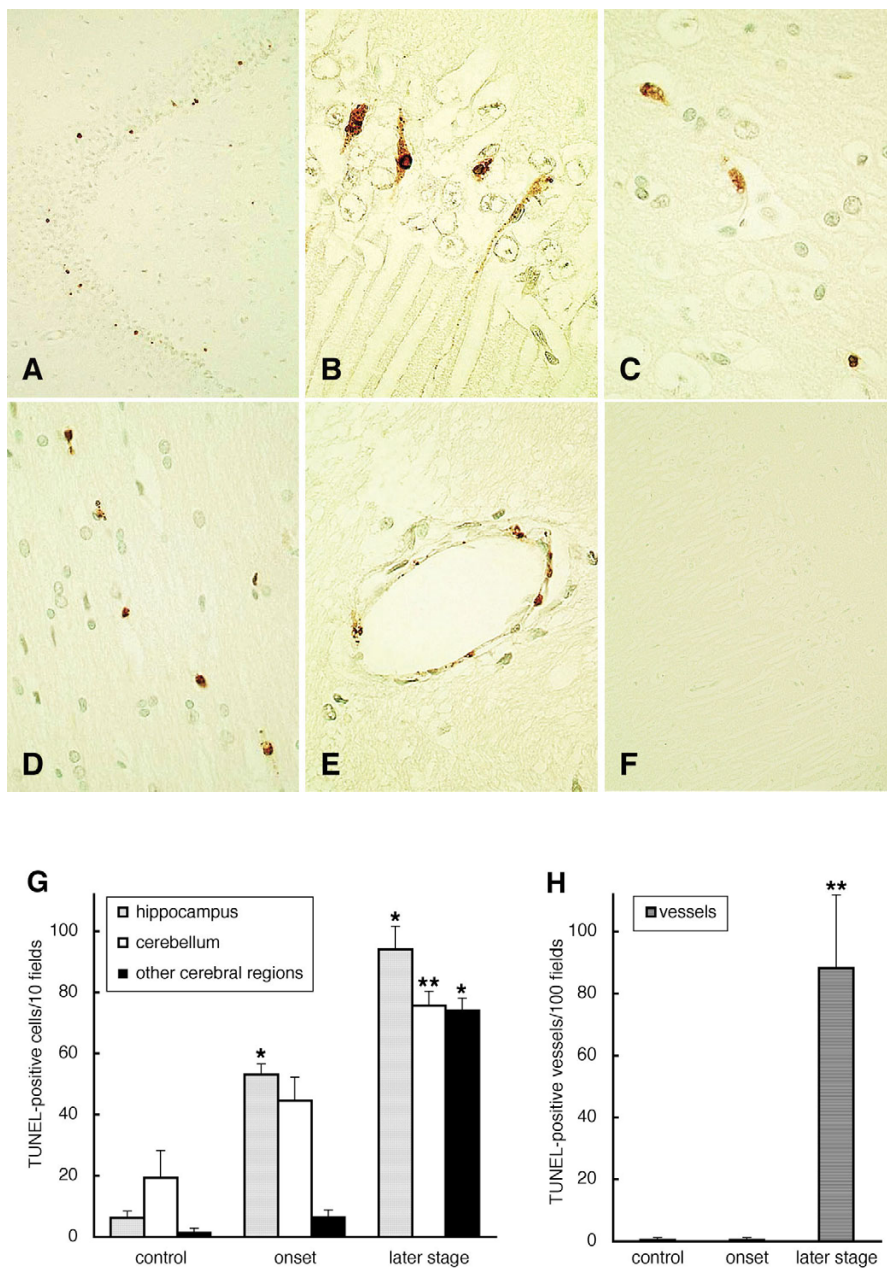


Figure 4

TUNEL assay of brain sections from rabbits treated with 2.5 µg/kg of Stx2. (A) Condensed dark brown cells were detected in the dentate gyrus of the hippocampus at the onset of paralysis. TUNEL-positive neurons showing shrunken cytoplasm, pycnotic nuclei, and/or apoptotic bodies increased at a later stage in the following other regions: CA1 of the hippocampus (B) and cerebral cortex (C). Apoptotic glial cells in pons (D) and small vessels (E) with condensed cytoplasm and apoptotic bodies were also observed at a later stage. (F) TUNEL assay without TdT showed no positive staining. (G) Quantitative evaluation of TUNEL-positive cells per 10 fields in the hippocampus, cerebellum, and other cerebral regions, including the basal ganglia, thalamus, and cerebral cortex, and (H) TUNEL-positive vessels per 100 fields in the cerebral parenchyma at the onset of neurological symptoms and at a later stage when compared with control rabbits treated with PBS(-) (n = 2 in each group). The number of apoptotic cells significantly increased in the hippocampus at both onset and a later stage, and in granular layers of the cerebellum and other cerebral regions at a late stage. TUNEL-positive vessels were significantly elevated at a later stage. *: P < 0.01 and **: P < 0.05. (Original magnification: (A) and (F) 200×, (B) 800×, (C) and (E) 600×, (D) 400×)

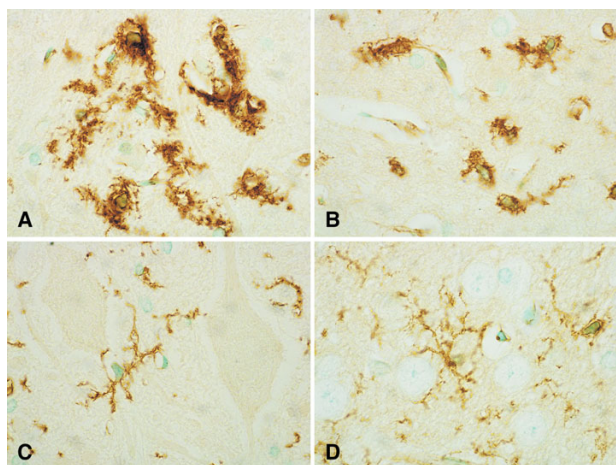


Figure 5
GSL I-B4 isolectin staining for microglia. In the rabbits treated with 2.5 $\mu\text{g}/\text{kg}$ of Stx2, a large number of microglia exhibited an ameboid form in and around the ischemic lesions in the lumbar cord gray matter (A) and extensively increased in the brain parenchyma, thalamus (B) at the onset of paralysis, when compared with the lumbar cord (C) and thalamus (D) of control rabbits injected with PBS(-), showing a ramified form of microglia. (Original magnification: 800 \times)

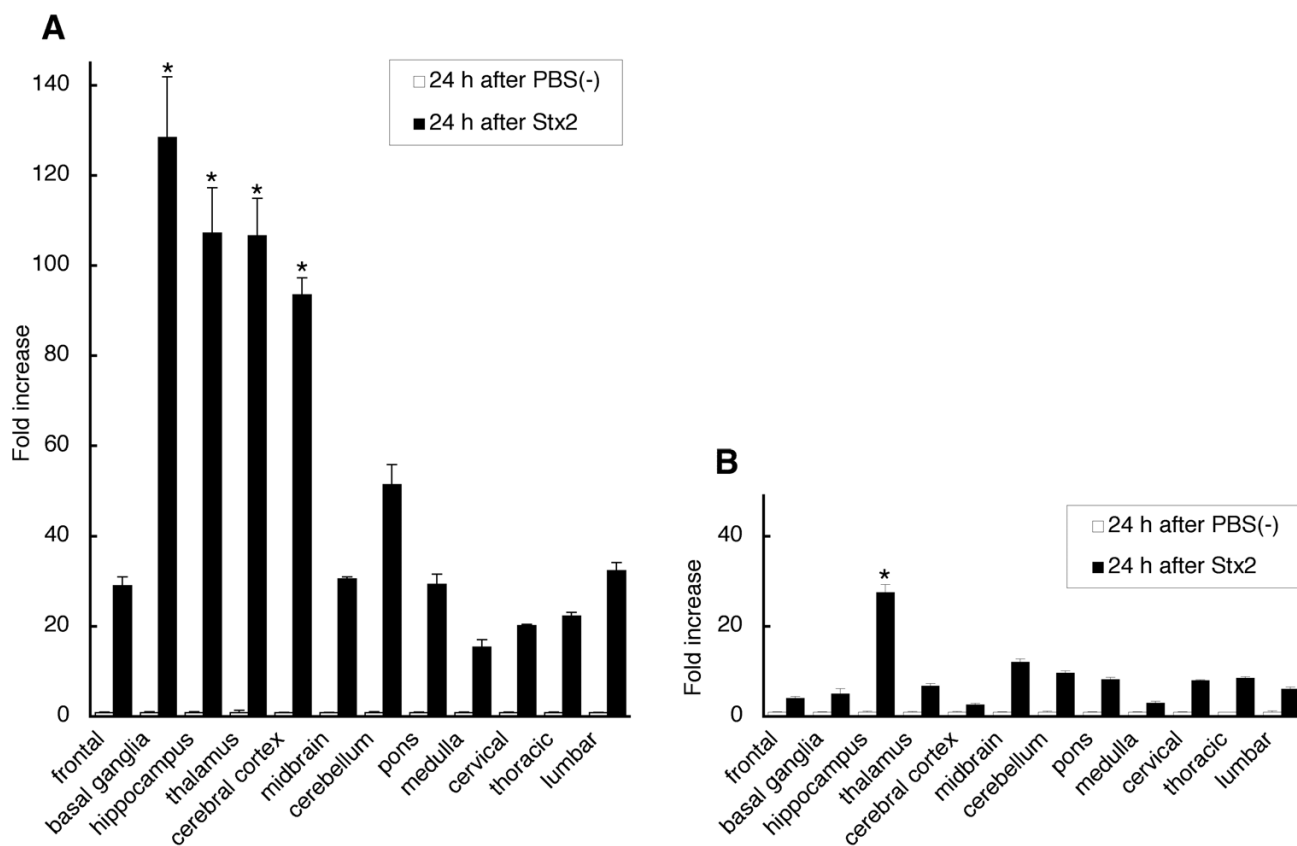
from those in the spinal cord although the primary action of Stxs was cytotoxicity against vascular endothelial cells expressing Gb3/CD77, not against neuronal cells, in both the spinal cord and brain.

Early studies showed that neuropathology, such as endothelial injury with thrombi and ischemic damage in rabbits treated with Stx1 or Stx2, was severe and extensive in the spinal cord but minimal in the brain [4,6]; this indicated specific binding of Stx1 to the endothelial cells of capillaries and vascular damage in the affected rabbit tissue [4]. These are in accordance with our results that neuropathological damage is markedly associated with regional distribution and cellular localization of Gb3/CD77 expression in the CNS parenchyma, indicating that the cytotoxic effects of Stx2 on endothelial cells was proportionate to the extent of Gb3/CD77 expression. Subsequent progression of acute neuronal injury in the spinal cord gray matter is mainly responsible for the paralysis that is the prominent clinical manifestation in the rabbit model treated with toxins.

Unlike the severe and massive ischemic insults in the spinal cord, the remarkable histopathology observed in the brain was due to neuronal cell death as evaluated by the TUNEL assay. Neuronal apoptosis was observed in both the dentate gyrus of the hippocampus and granular layers of the cerebellum at the onset of neurological symptoms,

thereafter, significantly increased at a later stage several days after onset in more cell subsets, such as the pyramidal neurons in the hippocampus, neurons in other regions, and glial cells in the white matter as well as in vascular endothelial cells in the cerebral parenchyma. Toxin binding was detected in ependymal cells and the myelin sheath as well as the endothelial cells in brain lesions of the rabbit injected with Stx2 [7], but not in the neurons [4,7]. Neuronal changes in a baboon exposed to a high level of Stx1 [35] and in a rabbit treated with Stx2 [36] were microscopically demonstrated. Further, Stx2 administered into the cerebroventricular space was detected in astrocyte and neuronal fibers in the rat corpus striatum, resulting in their ultrastructural alterations [37]. However, the mechanism by which toxin binding leads to neuronal damages has not been elucidated. Besides the brain endothelial cells, GB3/CD77 expression was not detected in either neurons or glial cells by the IFA. This suggests that Stxs might not directly exhibit essential cytotoxic action, i.e., protein synthesis inhibition, against neuronal cells. Accordingly, neuronal degeneration following Stx2 administration is very likely caused by indirect effects, rather than by direct cytotoxicity of the toxin against neuronal cells.

In the current study, immunoreactivity and morphological changes of microglia were increased as early as 12 h after Stx2 injection and TNF- α transcripts were markedly increased in the brain before onset of neurological symptoms. Most pathological changes in the CNS are accompanied by an involvement of glial cells, particularly microglia, which are activated at an early stage and change their morphology rapidly in response to even minor pathological conditions in the CNS [15,38]. We previously observed widespread activation of microglia in the brain parenchyma in acute fatal measles cases in which only endothelial cells of small vessels were infected with the measles virus [39]. This suggests that endothelial injury by Stx2 can also evoke microglial activation. Endogenous thrombin generated by vascular damage might contribute to activation of microglia [40]. Activated microglia, by inhibiting both the basal formation of new neurons and increased neurogenesis in response to brain insults, may contribute to the neurodegenerative processes [41]. Furthermore, activated microglia are known to produce pro-inflammatory cytokines, such as TNF- α and IL-1 β [15,23,38,40], which are observed long before significant neuronal death at the early phases of neuroinflammatory events [16]. TNF- α is shown to induce neurodegeneration directly, through signaling death pathway of TNF- α /p55 TNF receptor-1 in neurons [24,42] and oligodendrocytes [25] or through inducing activation of caspase-3 in a mixed neuro-glial culture system [43], furthermore, indirectly, through inhibiting receptor signaling for neuronal survival via the protective peptide insulin-like growth fac-

**Figure 6**

Real-time quantitative PCR study. TNF- α (**A**) and IL-1 β (**B**) transcripts in 12 regions of the rabbit CNS at 24 h after injection of PBS(-) as a calibrator (open bar: $1 \pm$ SD) or 2.5 μ g/kg Stx2 (closed bar: mean \pm SD). All data were normalized to the internal reference GAPDH amounts and expressed as an *n*-fold increase relative to normalized calibrator values in each region. Both TNF- α and IL-1 β mRNA levels were greatly up-regulated. In particular, TNF- α transcripts were significantly over-expressed in the cerebrum, basal ganglia, hippocampus, thalamus, and cerebral cortex. *: $P < 0.01$ compared to frontal region.

tor I [44] or through inducing microglial glutamate release in an autocrine manner [45]. Collectively, our observations that inflammatory responses, such as microglial activation and TNF- α overexpression, occurred in the brain of the rabbits at an early stage suggest that neuronal apoptosis and degeneration is probably triggered by neuroinflammation that is induced in response to primary endothelial injury by Stx2. The synergistic effects of TNF- α and IL-1 β , however, have been demonstrated in human fetal brain cell cultures [42], thus suggesting that IL-1 β , which showed a small increase in our animal model, might also participate in the neurodegenerative processes.

Previous studies have demonstrated that Stx1 induces apoptosis in the brain microvascular endothelial cells [46] in a dose- and time-dependent manner [11,47]. Toxins inhibit the expression of the anti-apoptotic Bcl-2 family member Mcl-1 in endothelial cells [12], and caspase inhibitors block apoptotic cell death [11,46,47]. Gb3/

CD77 expression on the membrane of these cells is required to activate the death signal cascade and enhance Bax expression [11]. Therefore, in contrast to neuronal cell death, endothelial apoptosis in the brain parenchyma is most likely Gb3/CD77-dependent and induced by the direct cytotoxic effects of Stx2. Moreover, *in vitro* studies have shown that pro-inflammatory cytokines such as TNF- α and IL-1 β markedly increased the Gb3/CD77 content of and Stx-binding to brain microvascular endothelial cells, resulting in the up-regulation of cytotoxicity [48-50] and apoptotic cell death [46].

There are no specific therapies to ameliorate the course of neurological involvement during STEC infection. However, treatment with nafamostat mesilate (6-amidino-2-naphthyl *p*-guanidinobenzoate dimethanesulfonate) significantly decreased the pro-inflammatory cytokine levels in the brain and changed the neuropathology in gnotobiotic mice infected with STEC O157:H7 [26]. Inhibition of

Stx1-induced TNF- α production with anisodamine (race-anisodamine hydrochloride) prolonged the survival time and decreased the lethality of mice injected with the toxin [51]. Suppressing neuroinflammatory responses generally [26,52] or neurotoxic molecules selectively [19,21,45] has recently been recognized as an effective therapeutic strategy for neurodegenerative diseases. Therefore, anti-inflammatory compounds or selective inhibitors may have therapeutic potential for Stx-induced neurological manifestation as well.

Conclusion

The Stx receptor Gb3/CD77 was expressed on endothelial cells in the brain parenchyma, but not on neurons or glial cells. Therefore, vascular damages and induction of endothelial apoptosis were very likely caused by direct cytotoxic action of Stx2. Apoptotic cell death of neurons and/or glial cells, however, may result from inflammatory responses in CNS following primary endothelial injury by Stx2; this is because microglial activation and significant up-regulation of TNF- α and IL-1 β transcripts occurs in the brain parenchyma of rabbits treated with Stx2. Collectively, these results suggest that inflammatory responses play a critical role in progression of neurological impairment during STEC infection; however, the expression of Gb3/CD77 in the human CNS still remains unclear.

Competing interests

The author(s) declare that they have no competing interests.

Authors' contributions

KT designed the experiments and carried out most of the lab work. AF and FI performed the histopathological evaluation, including a part of tissue staining. SS aided in quantitative and statistical analysis and edited the manuscript.

Acknowledgements

The authors thank Dr. Takashi Inoue for the neurological evaluation; Dr Wataru Habano for the technical advice; Ms. Kumi Furusawa, Ms. Sumiko Yaegashi, Ms. Ikuko Adachi, Mr. Yuji Shibata, and Mr. Shuichiro Hayashi for expert technical assistance; and Mr. Mitsutoshi Sasaki for the animal care. This work was supported by grants-in-aid for Advanced Medical Science Research by the Ministry of Science, Education, Sports, and Culture of Japan.

References

1. Strockbine NA, Marques LRM, Newland JW, Smith HW, Holmes RK, O'Brien AD: **Two toxin-converting phages from *Escherichia coli* O157:H7 strain 933 encode antigenically distinct toxins with similar biologic activities.** *Infect Immun* 1986, **53**:135-140.
2. Richardson SE, Karmali MA, Becker LE, Smith CR: **The histopathology of the hemolytic uremic syndrome associated with verocytotoxin-producing *Escherichia coli* infections.** *Hum Pathol* 1988, **19**:1102-1108.
3. Upadhyaya K, Barwick K, Fishaut M, Kashgarian M, Siegel NJ: **The importance of nonrenal involvement in hemolytic-uremic syndrome.** *Pediatrics* 1980, **65**:115-120.
4. Richardson SE, Rotman TA, Jay V, Smith CR, Becker LE, Petric M, Olivieri NF, Karmali MA: **Experimental verocytotoxemia in rabbits.** *Infect Immun* 1992, **60**:4154-4167.
5. Zoja C, Corna D, Farina C, Sacchi G, Lingwood C, Doyle MP, Padhye VV, Abbate M, Remuzzi G: **Verotoxin glycolipid receptors determine the localization of microangiopathic process in rabbits given verotoxin-1.** *J Lab Clin Med* 1992, **120**:229-238.
6. Barrett TJ, Potter ME, Wachsmuth IK: **Continuous peritoneal infusion of Shiga-like toxin II (SLT II) as a model for SLT II-induced diseases.** *J Infect Dis* 1989, **159**:774-777.
7. Fujii J, Kinoshita Y, Kita T, Higure A, Takeda T, Tanaka N, Yoshida S: **Magnetic resonance imaging and histopathological study of brain lesions in rabbits given intravenous verotoxin 2.** *Infect Immun* 1996, **64**:5053-5060.
8. Ling H, Boodhoo A, Hazes B, Cummings MD, Armstrong GD, Brunton JL, Read RJ: **Structure of the Shiga-like toxin I B₃-pentamer complexed with an analogue of its receptor Gb₃.** *Biochemistry* 1998, **37**:1777-1788.
9. Lingwood CA: **Role of verotoxin receptors in pathogenesis.** *Trends Microbiol* 1996, **4**:147-153.
10. O'Brien AD, Tesh VL, Donohue-Rolfe A, Jackson MP, Olsnes S, Sandvig K, Lindberg AA, Keusch GT: **Shiga toxin: biochemistry, genetics, mode of action and role in pathogenesis.** *Curr Top Microbiol Immunol* 1992, **180**:65-94.
11. Jones NL, Islur A, Haq R, Mascarenhas M, Karmali MA, Perdue MH, Zanke BW, Sherman PM: ***Escherichia coli* Shiga toxins induce apoptosis in epithelial cells that is regulated by the bcl-2 family.** *Am J Physiol Gastrointest Liver Physiol* 2000, **278**:G811-G819.
12. Erwert RD, Eiting KT, Tupper JC, Winn RK, Harlan JM, Bannerman DD: **Shiga toxin induces decreased expression of the anti-apoptotic protein Mcl-1 concomitant with the onset of endothelial apoptosis.** *Microb Pathog* 2003, **35**:87-93.
13. Utsunomiya I, Ren J, Taguchi K, Ariga T, Tai T, Ihara Y, Miyatake T: **Immunohistochemical detection of verotoxin receptors in nervous system.** *Brain Res Prot* 2001, **8**(2):99-103.
14. Streit WJ, Mrak RE, Griffin WST: **Microglia and neuroinflammation: a pathological perspective.** *J Neuroinflammation* 2004, **1**:14.
15. Kreutzberg GW: **Microglia: a sensor for pathological events in the CNS.** *Trends Neurosci* 1996, **19**:312-318.
16. Allan SM, Rothwell NJ: **Cytokines and acute neurodegeneration.** *Nat Rev Neurosci* 2001, **2**:734-744.
17. Muñoz-Fernández MA, Fresno M: **The role of Tumor necrosis factor, interleukin 6, interferon- γ and inducible nitric oxide synthase in the development and pathology of the nervous system.** *Prog Neurobiol* 1998, **56**:307-340.
18. Barone FC, Arvin B, White RF, Miller A, Webb CL, Willette RN, Lysko PG, Feuerstein GZ: **Tumor necrosis factor- α A mediator of focal ischemic brain injury.** *Stroke* 1997, **28**:1233-1244.
19. Combs CK, Kario JC, Kao S-C, Landreth GE: **β -amyloid stimulation of microglia and monocytes results in TNF α -dependent expression of inducible nitric oxide synthase and neuronal apoptosis.** *J Neurosci* 2001, **21**:1179-1188.
20. Patel NS, Paris D, Mathura V, Quadros AN, Crawford FC, Mullan MJ: **Inflammatory cytokine levels correlate with amyloid load in transgenic mouse models of Alzheimer's disease.** *J Neuroinflammation* 2005, **2**:9.
21. Hirsch EC, Breidert T, Rousset E, Hunot S, Hartmann A, Michel PP: **The role of glial reaction and inflammation in Parkinson's disease.** *Ann N Y Acad Sci* 2003, **991**:214-228.
22. Swarup V, Ghosh J, Duseja R, Ghosh S, Basu A: **Japanese encephalitis virus infection decrease endogenous IL-10 production: correlation with microglial activation and neuronal death.** *Neurosci Lett* 2007, **420**:144-149.
23. Wesselingh SL, Takahashi K, Glass JD, McArthur JC, Griffin JW, Griffin DE: **Cellular localization of tumor necrosis factor mRNA in neurological tissue from HIV-infected patients by combined reverse transcriptase/polymerase chain reaction in situ hybridization and immunohistochemistry.** *J Neuroimmunol* 1997, **74**:1-8.
24. Yang L, Lindholm K, Konishi Y, Li R, Shen Y: **Target depletion of distinct tumor necrosis factor receptor subtypes reveals hippocampal neuron death and survival through different signal transduction pathways.** *J Neurosci* 2002, **22**:3025-3032.
25. Akassoglou K, Bauer J, Kassiotis G, Pasparakis M, Lassmann H, Kollias G, Probert L: **Oligodendrocyte apoptosis and primary demyelination induced by local TNF/p55TNF receptor signaling in**

- the central nervous system of transgenic mice. **Models for multiple sclerosis with primary oligocendroglipathy.** *Am J Pathol* 1998, **153**:801-813.
26. Isogai E, Isogai H, Kimura K, Hayashi S, Kubota T, Fujii N, Takeshi K: **Role of tumor necrosis factor alpha in gnotobiotic mice infected with an Escherichia coli O157:H7 strain.** *Infect Immun* 1998, **66**:197-202.
 27. Yutsudo T, Nakabayashi N, Hirayama T, Takeda Y: **Purification and some properties of a Vero toxin from Escherichia coli O157:H7 that is immunologically unrelated to Shiga toxin.** *Microb Pathog* 1987, **3**:21-30.
 28. Oishi H, Takaoka A, Hatayama Y, Matsuo T, Sakata Y: **Automated limulus amebocyte lysate (LAL) test for endotoxin analysis using a new Toxinometer ET-201.** *J Parenter Sci Technol* 1985, **39**:194-199.
 29. Nitatori T, Sato N, Waguri S, Karasawa Y, Araki H, Shibani K, Kom-inami E, Uchiyama Y: **Delayed neuronal death in the CA1 pyramidal cell layer of the gerbil hippocampus following transient ischemia is apoptosis.** *J Neurosci* 1995, **15**:1001-1011.
 30. Takahashi K, Wesselingh SL, Griffin DE, McArthur JC, Johnson RT, Glass JD: **Localization of HIV-1 in human brain using polymerase chain reaction/in situ hybridization and immunohistochemistry.** *Ann Neurol* 1996, **39**:705-711.
 31. Simpson DAC, Feeney S, Boyle C, Stitt AV: **Retinal VEGF mRNA measured by SYBR green I fluorescence: A versatile approach to quantitative PCR.** *Mol Vis* 2000, **6**:178-183.
 32. Reno C, Boykiw R, Martinez ML, Hart DA: **Temporal alterations in mRNA levels for proteinases and inhibitors and their potential regulators in the healing medial collateral ligament.** *Biochem Biophys Res Commun* 1998, **252**:757-763.
 33. Murata T, Yamawaki H, Hori M, Sato K, Ozaki H, Karaki H: **Hypoxia impairs endothelium-dependent relaxation in organ cultured pulmonary artery.** *Eur J Pharmacol* 2001, **421**:45-53.
 34. Wu AM, Wu JH, Singh T, Lai L-J, Yang Z, Herp A: **Recognition factors of Ricinus communis agglutinin I (RCA₁).** *Mol Immunol* 2006, **43**:1700-1715.
 35. Taylor FB Jr, Tesh VL, DeBault L, Li A, Chang ACK, Kosanke SD, Pysker TJ, Siegler RL: **Characterization of the baboon responses to Shiga-like toxin. Descriptive study of a new primate model of toxic responses to Stx-1.** *Am J Pathol* 1999, **154**:1285-1299.
 36. Mizuguchi M, Tanaka S, Fujii I, Tanizawa H, Suzuki Y, Igarashi T, Yamanaka T, Takeda T, Miwa M: **Neuronal and vascular pathology produced by verocytotoxin 2 in the rabbit central nervous system.** *Acta Neuropathol* 1996, **91**:254-262.
 37. Goldstein J, Loidl CF, Creydt VP, Boccoli J, Ibarra C: **Intracerebroventricular administration of Shiga toxin type 2 induces striatal neuronal death and glial alterations: An ultrastructural study.** *Brain Res* 2007, **1161**:106-115.
 38. Aloisi F: **Immune function of microglia.** *Glia* 2001, **36**:165-179.
 39. Esolen LM, Takahashi K, Johnson RT, Vaisberg A, Moench TR, Wesselingh SL, Griffin DE: **Brain endothelial cell infection in children with acute fatal measles.** *J Clin Invest* 1995, **96**:2478-2481.
 40. Lee DY, Park KW, Jin BK: **Thrombin induces neurodegeneration and microglial activation in the cortex in vivo and in vitro: Proteolytic and non-proteolytic actions.** *Biochem Biophys Res Commun* 2006, **346**:727-738.
 41. Ekdahl CT, Claassen J-H, Bonde S, Kokaia Z, Lindvall O: **Inflammation is detrimental for neurogenesis in adult brain.** *Proc Natl Acad Sci USA* 2003, **100**:13632-13637.
 42. Chao CC, Hu S, Ehrlich L, Peterson PK: **Interleukin-1 and tumor necrosis factor- α synergistically mediate neurotoxicity: Involvement of nitric oxide and of N-methyl-D-aspartate receptors.** *Brain Behav Immun* 1995, **9**:355-365.
 43. Zhao X, Bausano B, Pike BR, Newcomb-Fernandez JK, Wang KKW, Shohami E, Ringger NC, DeFord SM, Anderson DK, Hayes RL: **TNF- α stimulates caspase-3 activation and apoptotic cell death in primary septo-hippocampal cultures.** *J Neurosci Res* 2001, **64**:121-131.
 44. Venters HD, Tang Q, Liu Q, VanHoy RW, Dantzer R, Kelley KW: **A new mechanism of neurodegeneration: A proinflammatory cytokine inhibits receptor signaling by a survival peptide.** *Proc Natl Acad Sci USA* 1999, **96**:9879-9884.
 45. Takeuchi H, Jin S, Wang J, Zhang G, Kawanokuchi J, Kuno R, Sonobe Y, Mizuno T, Suzumura A: **Tumor necrosis factor- α induces neurotoxicity via glutamate release from hemichannels of activated microglia in an autocrine manner.** *J Biol Chem* 2006, **281**:21362-21368.
 46. Ergonul Z, Hughes AK, Kohan DE: **Induction of apoptosis of human brain microvascular endothelial cells by Shiga toxin I.** *J Infect Dis* 2003, **187**:154-158.
 47. Pijpers AHJM, Van Setten PA, Van Den Heuvel LPWJ, Assmann KJM, Dijkman HBPM, Pennings AHM, Monnens LAH, Van Hinsbergh VWM: **Verocytotoxin-induced apoptosis of human microvascular endothelial cells.** *J Am Soc Nephrol* 2001, **12**:767-778.
 48. Ramegowda B, Samuel JE, Tesh VL: **Interaction of Shiga toxins with human brain microvascular endothelial cells: Cytokines as sensitizing agents.** *J Infect Dis* 1999:1205-1213.
 49. Eisenhauer PB, Chaturvedi P, Fine RE, Ritchie AJ, Pober JS, Cleary TG, Newburg DS: **Tumor necrosis factor alpha increases human cerebral endothelial cell Gb₃ and sensitivity to Shiga toxin.** *Infect Immun* 2001, **69**:1889-1894.
 50. Stricklett PK, Hughes AK, Ergonul Z, Kohan DE: **Molecular basis for up-regulation by inflammatory cytokines of Shiga toxin I cytotoxicity and globotriaosylceramide expression.** *J Infect Dis* 2002, **186**:976-982.
 51. Zhang H-M, Ou ZL, Gondaira F, Ohmura M, Kojio S, Yamamoto T: **Protective effect of anisodamine against Shiga toxin-I: Inhibition of cytokine production and increase in the survival of mice.** *J Lab Clin Med* 2001, **137**:93-100.
 52. Qian L, Xu Z, Zhang W, Wilson B, Hong JS, Flood PM: **Sinomenine, a natural dextrorotatory morphinan analog, is anti-inflammatory and neuroprotective through inhibition of microglial NADPH oxidase.** *J Neuroinflammation* 2007, **4**:23.

Publish with **BioMed Central** and every scientist can read your work free of charge

"BioMed Central will be the most significant development for disseminating the results of biomedical research in our lifetime."

Sir Paul Nurse, Cancer Research UK

Your research papers will be:

- available free of charge to the entire biomedical community
- peer reviewed and published immediately upon acceptance
- cited in PubMed and archived on PubMed Central
- yours — you keep the copyright

Submit your manuscript here:
http://www.biomedcentral.com/info/publishing_adv.asp

